

Characterization of Tapioca Starch Biopolymer Composites Reinforced with Micro Scale Water Hyacinth Fibers

Hairul Abrol,* Maro Hagabean Dalimunthe, Joko Hartono, Rice Putra Efendi, Mochamad Asrofi, Eni Sugiarti, S. M. Sapuan, Ji-Won Park, and Hyun-Joong Kim

This paper reports on the properties of microscale water hyacinth fiber pulp (WHF) filled tapioca starch biopolymer (TSB) composites. The volume fraction of WHF in the TSB matrix is varied, that is, 1%, 3%, 5%, and 10%. A casting method is used for making sample films of the biocomposites. Scanning electron microscopy (SEM) of the fracture surface of the biocomposite for the tensile samples displays good fiber distribution in the matrix, and interface bonding between WHF and TSB. The 10% fiber biocomposite delivers the highest value of tensile strength (TS) of 6.68 MPa, and tensile modulus (TM) of 210.95 MPa; however, this combination also has the lowest fracture strain of 7.30%. In this case, there was 549% improvement of TS and 973% of TM in comparison to TSB. The biocomposite with 10% WHF content also shows the highest thermal resistance and the lowest moisture absorption. It shows potential for future commercial applications.

1. Introduction

In last two decades, attention has been given to the development of starch-based thermoplastics as a way of reducing non-degradable

Prof. H. Abrol, M. H. Dalimunthe, J. Hartono, R. P. Efendi, M. Asrofi
Department of Mechanical Engineering
Andalas University
Padang 25163, Sumatera Barat, Indonesia
E-mail: abrol@ft.unand.ac.id

Dr. E. Sugiarti
Laboratory of High Temperature Coating
Research Center for Physics Indonesian Institute of Sciences (LIPI)
Serpong, Jakarta 15314, Indonesia

Prof. S. M. Sapuan
Faculty of Engineering
Department of Mechanical and Manufacturing Engineering
Universiti Putra Malaysia
Serdang 43400 UPM Selangor, Malaysia

Prof. S. M. Sapuan
Laboratory of Biocomposite Technology
Institute of Tropical Forestry and Forest Products (INTROP)
Universiti Putra Malaysia
Serdang 43400 UPM Selangor, Malaysia

Dr. J.-W. Park, Prof. H.-J. Kim
Laboratory of Adhesion and Bio-Composites
Program in Environmental Materials Science
Research Institute for Agriculture and Life Sciences
Seoul National University
151-921 Seoul, Republic of Korea

DOI: 10.1002/star.201700287

synthetic polymer use.^[1] These thermoplastics are environmentally friendly, cheap to produce from widely available raw materials and biodegradable.^[2] The cassava or tapioca plant is one extensively researched source of starch because it grows abundantly in tropical countries like Indonesia. This plant has a high water content along with starch and celluloses fibers.^[3] However, compared with conventional synthetic thermoplastics, tapioca starch thermoplastics are brittle, have poor mechanical properties, and are water sensitive.^[4] Extensive research has been conducted to attempt to enhance these properties in recent years.^[3,5–7] Brittleness has been reduced by mixing in a plasticizer such as glycerol.^[8] To increase tensile strength and water resistance, fillers obtained from natural fibers have been added to starch-based biopolymers to produce biocomposites.^[5,9,10] Chen et al.^[11] reported an improvement of mechanical

properties, thermal, and moisture resistance of biocomposites that included cellulose nanoparticles from natural sources. Some other recent results have indicated significant improvement of some properties of starch-based biocomposites if they are reinforced by micro-sized natural fibers.^[12–14]

Generally, the natural fiber has chemical compositions consisting of celluloses, hemicelluloses, and lignin.^[11] The strength of the fibers depends on the cellulose content.^[15] If this is high, the mechanical properties are improved.^[16] One possible natural fiber reinforcement in starch-based composites is WHF which has a high cellulose content of 30–50%.^[17] Water hyacinths reproduce prolifically in the tropics, creating problems in the environment as they block irrigation channels. They are easily harvested as they float on the water surface. Commercial use of the plant is still limited, however. Therefore, considering its high cellulose content, it could be used as a reinforcement material for biocomposites.^[18]

Size of the reinforcing fibers affect the mechanical properties of a starch-based thermoplastic.^[4] A decrease in fiber diameter improves mechanical properties and resistance to moisture absorption.^[4] Intensive studies have been conducted to improve the surface area ratio between fibers and the matrix interface by reducing the diameter of the fibers.^[19] Nano-crystals of ramie cellulose in a bioplastic of wheat starch has been shown to improve the properties of the biocomposite.^[5] Such cellulose nano-crystals from plant sources can be produced mechanically

or chemically.^[20–24] However, producing nano-sized dimension fibers is expensive and can use environmentally damaging chemicals. It is economically advantageous if micro-sized fibers from abundantly available plants could be utilized as the reinforcing material for starch-based thermoplastics. Therefore it is necessary to develop methods to lower the cost and optimize the performance of bio-based products so they can be used to create efficient packaging materials that are environmentally friendly, safe, and preserve food quality.^[25]

Some previous work using WHF has been published.^[9,18,26–29] However, as far as we are aware, there are no previous studies investigating the microscale effects of WHF on the physical and mechanical properties of starch tapioca based thermoplastics. Therefore, this research was designed to study the properties of this combination. Mechanical properties, thermal resistance, moisture absorption, FTIR, XRD, SEM fracture surface of the studied samples were measured. Results of this investigation could form a basis for further research to provide a better understanding of the properties of this biocomposite and the potential development of a commercially attractive solution to a pressing environmental problem.

2. Experimental Section

2.1. Extraction of WHF

Extraction of WHF was conducted as in previous research.^[9] The fiber was extracted from freshwater hyacinths growing in a local swamp in 50 Kota district, Indonesia, cut into 1 cm lengths and cleaned with fresh water. Then, it was placed in a plastic covered shelter under sunlight for 5 days to dry. The dried WHF samples were mixed with a 25% NaOH solution and placed in a digester for 6 h at about 130 °C, two bars. The pulp was neutralized by water until pH 7, blended by a mixer for 10 min then screened by using a printing screen with T61 mesh. The wet pulp was then solar dried. The average diameter of the dried fiber was $2.96 \pm 0.52 \mu\text{m}$.

2.2. Measuring Chemical Compositions

The cellulose, lignin, and hemicellulose composition of WHF were determined. Cellulose and hemicellulose content was measured using the Technical Association of the Pulp and Paper Industry (TAPPI) standard T9M-54, and the lignin content was tested by using TAPPI T13M-54. For the sake of conciseness, these procedures are not explained in this paper.

2.3. Preparation of Biocomposites

The tapioca powder used for this research was a commercial product branded “Cap Pak Tani”, bought in a local market. The content of water, amylose, and amylopectin in the powder was 19, 15, and 85%, respectively. Tapioca starch bioplastic (TSB) was processed by mixing 1 g WHF with 140 mL of water. Then 10 g of tapioca powder and 3 mL of glycerol were added to the mixture which was then mixed with a (Daihan HG 15D-Set A)

homogenizer for 5 min at 5000 rpm. The solution was gelatinized using a magnetic stirrer at 150 °C, 500 rpm for 18 min. Finally, the gelatinizing biocomposite was poured into a rectangular glass mold and placed in a Universal drying oven (Mettmert UN-55) at 50 °C for 20 h. Samples for study were released from the mold after 24 h at room temperature.

2.4. Thermal Gravimetric Analyzing (TGA/DTG), Differential Scanning Calorimetry (DSC)

Measurement of the TGA/DTG and DSC was performed using a thermogravimetric analyzer (TGA/DSC1 equipment from Mettler Toledo). For TGA/DTG, a sample of about 7 mg was heated from 25 to 600 °C at $10^\circ\text{C min}^{-1}$, for DSC from room temperature to 250 °C at $10^\circ\text{C min}^{-1}$.

2.5. Moisture Absorption

Films with a dimension of $1 \times 1.5 \text{ cm}$ were dried in an oven (Universal Oven Mettmert UN-55) until constant weight then stored in a closed chamber with 99% relative humidity (RH) for 10 h. The samples were taken out and weighed on a precision balance to the nearest 0.1 mg (Kenko). The moisture absorption in the sample was calculated as a percentage from the difference between dried weight and wet weight divided by dried weight.^[27]

2.6. Tensile Testing

A Com-Ten 95T Series testing machine was used for measuring the tensile strength of all samples at 3 mm min^{-1} and room temperature 14 days after samples were released from the mold. Five repeats for each fiber percentage were conducted using ASTM D638 type I Standard test.^[30] Maximum force on the sample was divided by average cross-section area to obtain tensile strength. In order to obtain average cross-section area accurately, thickness and width were measured at ten different location points using a dial indicator micrometer to $1 \mu\text{m}$ accuracy. Tensile modulus was automatically derived by the tensile equipment as the slope of the linear region of the stress-strain curve. The strain of a sample was measured as the fracture strain.

2.7. XRD Testing

X-ray diffraction of the film was performed by using PANalytical Xpert PRO at 25 °C, 40 kV, and 30 mA. The samples were scanned from $2\theta = 3$ to 40° . Crystal size (L) was calculated using Equation (1):

$$L = k \cdot \lambda / (B \cos 2\theta) \quad (1)$$

where the values of k and λ were 0.89, 1.54, respectively. The value of B was measured from full width at half maximum of XRD pattern peak (FWHM) multiplied by $\pi/180$. The crystallinity index (CI) was measured by using Equation (2):^[31]

$$CI (\%) = (I_{200} - I_{am}) / I_{200} \times 100 \quad (2)$$

where I_{200} is the intensity of the peak corresponding to cellulose I, and I_{am} is the intensity of the peak of the amorphous fraction.

2.8. FTIR Characterization

The FTIR characterization was performed by using “The PerkinElmer Frontier.” The aim of FTIR characterization was to identify the state of the functional groups of the TSB and the TSB/WHF composite. The sheet film from the dried samples was scanned at the frequency range of 4000–600 cm^{-1} .

2.9. SEM Observation

Observation of the fracture surface of all tested samples was performed by using SEM (Hitachi 3400 N series) at 15 kV.

3. Results and Discussion

3.1. Chemical Composition of WHF

Chemical composition of natural fibers depends on growing location, age, temperature, and humidity.^[27] The WHF studied came from local sources, and its chemical composition is reported in Table 1. The composition of the WHF pulp was changed after processing. Before treatment, the WHF pulp had high lignin (4.1%) and hemicellulose (20.6%) content which decreased after digesting and blending for 10 min to 3.9% and 3.5%, respectively. Meanwhile, the cellulose content became more dominant in the treated WHF sample being 67%.

3.2. Thermogravimetric Analysis (TG) and Derivative of TGA (DTG)

Thermal degradation and decomposition of the present samples were observed to measure the relationship between thermal properties and differences in chemical composition. Figure 1a shows the TG curve of thermal weight loss, and Figure 1b is the DTG curve of samples as a function of rising temperature. The TG curve is composed of three main sections that have also been observed in previous studies.^[11,15] Up until 100 °C, the sample displays a slight loss of weight due to evaporation of water.^[3,32] This small amount of dehydration up until about 100 °C was also confirmed by the DTG curve (Figure 1b). As the temperature reaches the range of 250–340 °C,

Table 1. Chemical compositions in the untreated and treated WHF pulp

	Lignin [%]	Hemicellulose [%]	Cellulose [%]
Untreated	4.1	20.6	42.8
Treated WHF pulp	3.9	3.5	67.0

the TG curve indicates maximum decomposition of the sample probably attributable to oxidation of the partially decomposed starch as well as fiber degradation.^[33,34] Above 300 °C, the highest rate of decomposition is observed for the TSB. The rate of weight loss for the biocomposite samples containing WHF was lower than for the pure TSB. This was also observed in a previous study.^[35] The maximum thermal resistance was measured on the 10% WHF biocomposite which also displayed the highest CI of all tested samples as evidenced by the XRD diffraction discussed later in this present paper. The greater crystalline structure led to high resistance to heat and an increase in maximum temperature for thermal degradation as shown in Table 2.^[36] This phenomenon was similar to a previous report.^[37] Another factor that could also improve the thermal stability of the biocomposites is good interface bonding between TSB and WHF that led to strong hydrogen bonding, thus reducing the weight loss in the sample.^[36,38,39] This is consistent with FTIR curve (Figure 2) that shows shifting of the wave number of the biocomposite as evidence of good interface bonding.

3.3. FTIR Spectra

Figure 2 exhibits the FTIR spectra of the studied samples along with an untreated WHF control. These are similar to the FTIR spectrum published previously.^[27] After processing in the digester and blending 10 min the functional group of the WHF had a changed wave number position. Untreated WHF exhibits a broad spectrum and O–H stretching at wave number 3344.5 cm^{-1} . After boiling with 25% NaOH and blending 10 min, the O–H functional group shifted to 3283.8 cm^{-1} . Previous research reported that decrease in the wave number of O–H stretching could be attributed to lower force from electron delocalization.^[40] The C–H stretching data corresponds to the cellulose and hemicellulose component.^[41] After the treatment, these wave numbers were shifted from 2910.4 to 2920.9 cm^{-1} . The absorption area at 1253.9 cm^{-1} corresponds to a C–O–C functional group. After chemical and mechanical treatment, the C–O–C functional group disappeared (Figure 2b). Peaks in the wavenumber from 1037.6 to 1017.3 cm^{-1} corresponding to the C–O functional group related to the cellulose component shifted after chemical and mechanical treatment. The continuing presence of C–O functional groups proves that the cellulose component was not eliminated by alkali treatment.^[41] Meanwhile, TSB has an O–H functional group at wavenumber 3293 cm^{-1} (Figure 2c). After addition of 1, 3, 5, and 10% WHF to TSB, the O–H band shows a significant shifting. For example, the O–H functional group of 1% WHF biocomposite shifted to 3295 cm^{-1} as shown in Figure 2d. This shift is strong evidence for the formation of hydrogen bonds between WHF and the TSB matrix.^[42,43] The O–H functional groups were reduced as the amount of WHF fiber increased leading to a decrease in the ability of the O–H functional groups to bind with water resulting in a more hydrophobic biocomposite.

3.4. X-Ray Diffraction

X-ray diffraction was used to measure changes in the crystalline structure. Figure 3 shows XRD patterns for TSB (a), WHF (b), and

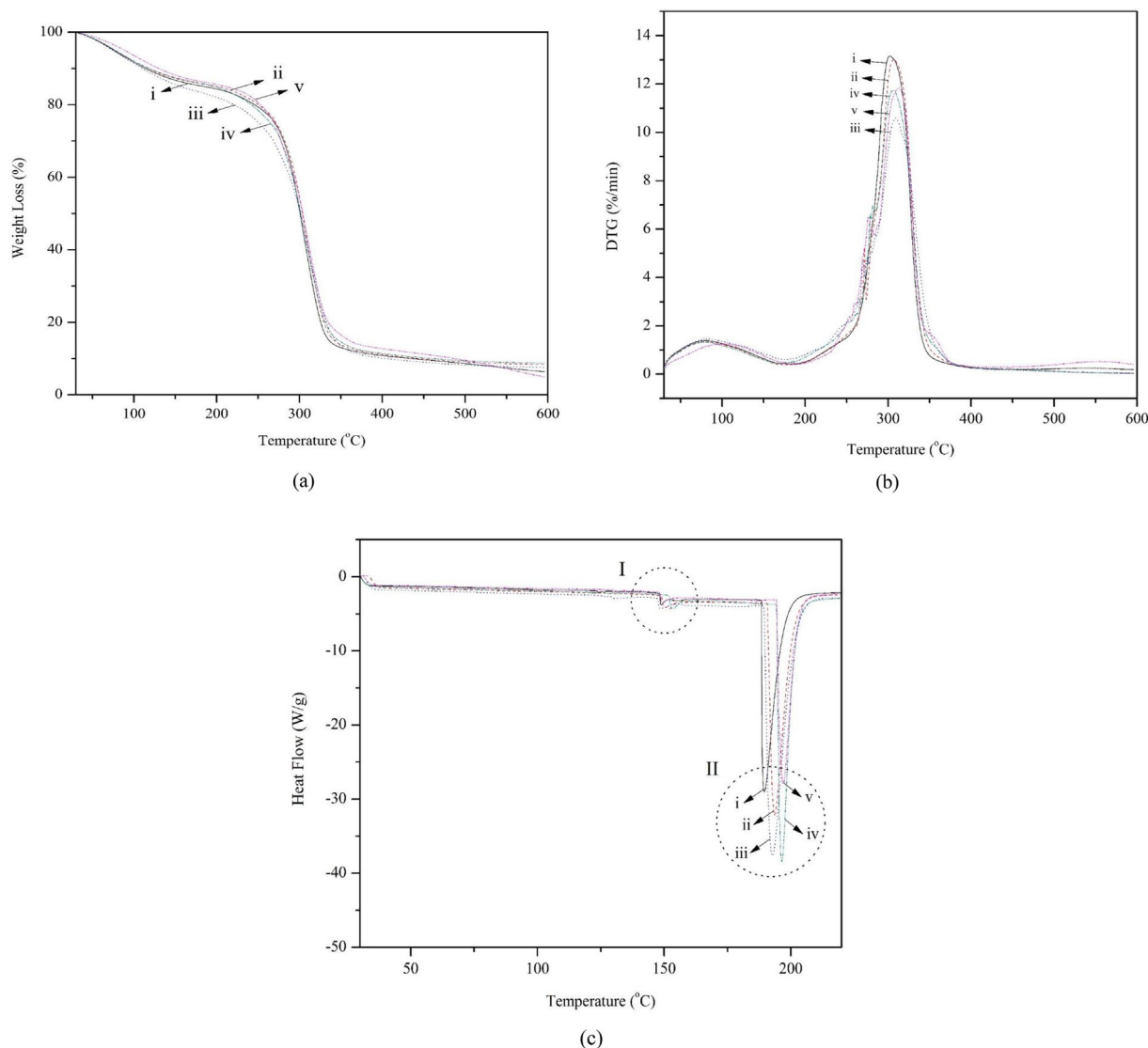


Figure 1. Curve of a) TG, b) DTG, and c) DSC for (i) TSB, (ii) 1% WHF in TSB, (iii) 3% WHF in TSB, (iv) 5% WHF in TSB, (v) 10% WHF in TSB.

WHF-TSB composites (c-d), meanwhile **Table 3** shows crystallinity index (CI) and the crystal system of all tested samples. The XRD pattern of WHF exhibits a sharp peak at a high scattering angle that indicates a high crystallinity index (CI).^[36] The CI of WHF peaked at 59.56% (Figure 3). The TSB shows a broad diffraction pattern

and a peak at a low scattering angle which can be attributed to high amorphous content and small crystal size.^[7] The CI of TSB was 10.9%. This explains why increases in WHF content in the TSB results in improvement of the CI of the resulting biocomposite as shown in Table 3. The highest CI was measured in the 10% WHF biocomposite. A high CI in a biocomposite is correlated with improved tensile properties, so it is expected that addition of WHF results in an enhancement of the TSB based biocomposite tensile properties.^[36,43]

Table 2. Crystallization (T_c), melting temperature (T_m), and melting enthalpy (H_m) of the samples from **Figure 1c**.

Sample	I		II		
	T_c [°C]	DSC [W g ⁻¹]	T_m [°C]	DSC [W g ⁻¹]	H_m [J g ⁻¹]
TSB	148.8	-3.8	189.6	-29.0	174
1%WHF in TSB	149.8	-4.0	193.5	-32.2	178
3%WHF in TSB	148.5	-4.3	192.7	-37.7	203
5%WHF in TSB	153.7	-4.2	196.5	-38.4	155
10%WHF in TSB	149.4	-3.5	197.0	-27.9	153

3.5. Moisture Absorption

Figure 4 shows average moisture absorption (MA) of samples with different fiber content as a function of time. There were five repeats for each fiber content tested. In the beginning, MA for all samples is similar and high due to the large difference in relative humidity between the sample and humid environment in the

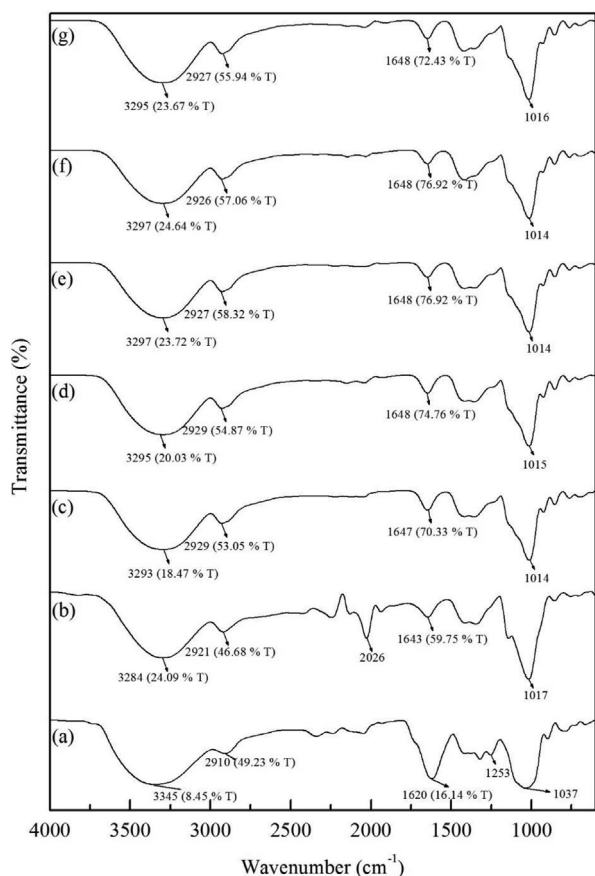


Figure 2. FTIR spectra for the studied samples of (a) untreated 100% WHF (b) treated 100% WHF (c) TSB (d) 1% WHF (e) 3% WHF (f) 5% WHF (g) 10% WHF in TSB matrix.

chamber. After time in the chamber, the rate of MA decreases toward a saturation point. It was noted that achievement of the saturation point for TSB took longer than for the biocomposite. Furthermore, MA of the biocomposite was lower than TSB and

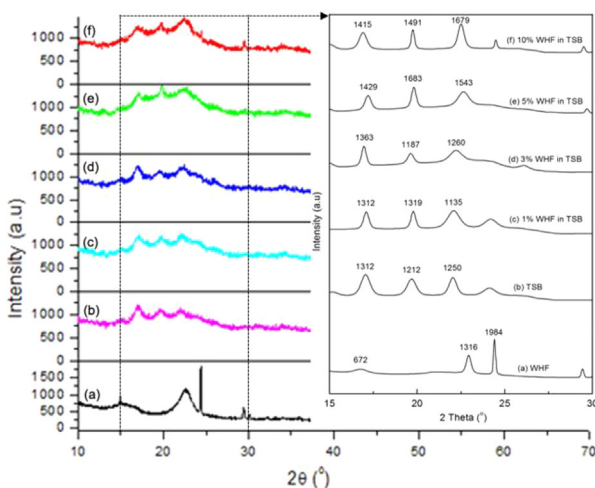


Figure 3. XRD patterns of six studied samples.

Table 3. Crystallinity index, crystal system, and compound of WHF, TSB, and biocomposite.

Sample	L [Å]	d [Å]	Crystallinity index [%]	Crystal system	Compound
WHF	57.25	3.93	59.56	Monoclinic	Cellulose-I β
TSB	68.99	4.03	10.90	Monoclinic	Cellulose
1% WHF in TSB	60.69	4.00	11.98	Anorthic	Cellulose-I α
3% WHF in TSB	60.18	4.00	14.26	Monoclinic	Cellulose-I β
5% WHF in TSB	59.92	3.98	12.08	Monoclinic	Cellulose-I β
10% WHF in TSB	59.43	3.95	17.36	Monoclinic	Cellulose-I β

tended to decrease as fiber content increased. This confirms that WHF used in the present study was less hygroscopic than the starch due to the higher degree of molecular order which results in improved barrier properties.^[44] After 10 h in the humid chamber, the lowest MA value was 26.8% for the 10% fiber biocomposite and highest at 32.6% for the TSB. Increasing WHF content in the TSB resulted in a more hydrophobic biocomposite presumably due to strong hydrogen bonding between WHF and TSB resulting in lower diffusivity of water molecules into the sample.^[8,45] This is reinforced by observation of the SEM fracture surface (Figure 5d).

3.6. Mechanical Properties

Figure 6 shows the tensile strength (TS) versus strain curve of individual samples with differing WHF content. As predicted from the CI results (see Table 3), pure TSB displayed a low TS and tensile modulus (TM), and the highest fracture strain. As fiber content increased, TS and TM values increased, and fracture strain decreased indicating that fiber strengthens the biocomposite but causes to become more brittle. Average values of TS, TM, and fracture strain versus the various WHF contents

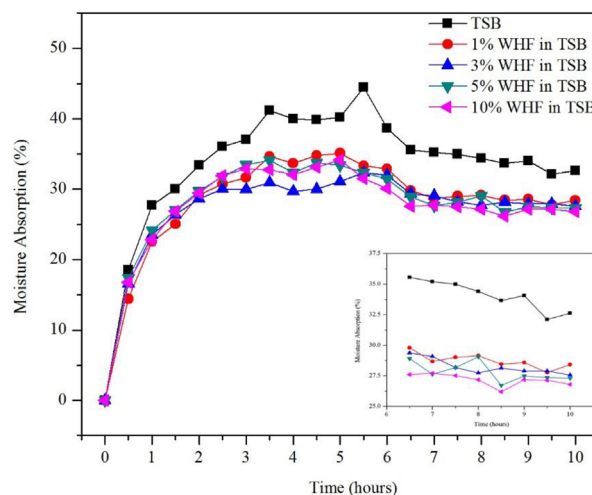


Figure 4. Performance of moisture absorption for TSB, and biocomposite. Average value from five repeats shown.

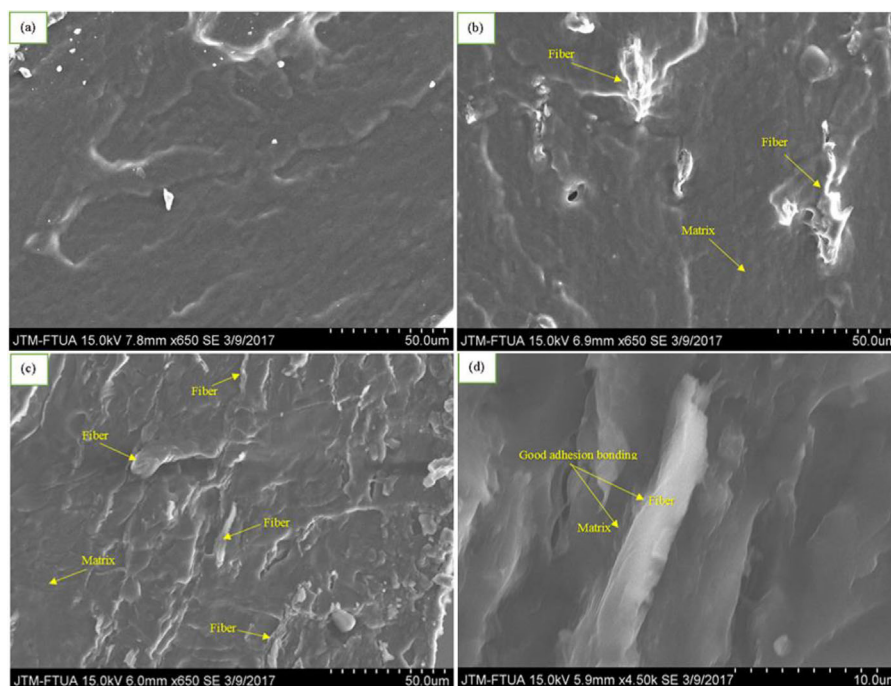


Figure 5. SEM photograph of a) TSB matrix b) 1% WHF in TSB matrix c) 10% WHF in TSB matrix d) good adhesion bonding of WHF in TSB matrix.

in TSB are displayed with error bars in **Figure 7a-c**, respectively. These confirm that both the TS and TM improved as fiber content increased, but fracture strain decreased. Average highest values for TS and TM of the 10% WHF biocomposite were 6.7 and 210.9 MPa, respectively. While this biocomposite was the strongest, it also had the lowest fracture strain of 3.7%. Hence, the addition of 10% WHF increased TS by 549%, and TM by 973% in comparison to TSB. Improvement of these mechanical properties may be due to the fact that the WHF was well distributed in the TSB so reinforced the biocomposite against the

applied external tensile load. Good interface bonding between WHF and TSB as shown in **Figure 5d** may also contribute to increases in TS and TM values of the biocomposites.

Similar improvement of mechanical properties with increases in fiber content has been observed in previous studies.^[15,42,46,47] The strength of this WHF/Tapioca bioplastic exceeds that of Zong-qiang et al.^[12] who used okara micro fiber as a reinforcement. Maximal tensile strength was less than half the value obtained in this study at 3.13 MPa when a 10% fraction of this fiber was used in a corn starch-based bioplastic. The superior performance of the bioplastic in this study is related to the smaller diameter of the WHF fibers, about $2.96 \pm 0.52 \mu\text{m}$ compared to $177 \mu\text{m}$ for the okara fibers.

3.7. SEM Photograph

The SEM photograph of pure TSB (**Figure 5a**) shows a smooth fracture surface. In comparison, the SEM photographs of biocomposites with various WHF content (**Figure 5b,c**) show rougher fracture surfaces due to the fiber content. As shown in **Figure 5b,c**, the fibers in the TSB matrix were uniformly distributed, and there was no agglomeration of the fibers observed. Agglomeration could reduce the mechanical properties of the biocomposite. The higher WHF content in the TSB improves the possibility of reinforcing fibers withstanding the external load, creating increases in the mechanical properties of the sample. Furthermore, an enlargement of the fracture surface in **Figure 5d** shows no gap between fibers and the matrix indicating good interfacial bonding. This is to be expected due to the similarity of the polysaccharide structures of cellulose and starch.^[48] Strong adhesion bonding effectively transfers applied

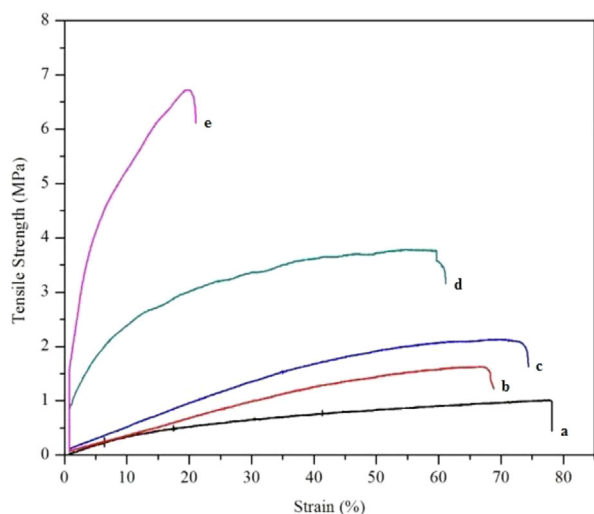


Figure 6. Tensile strength of individual sample a) TSB, b) 1% WHF in TSB, c) 3% WHF in TSB, d) 5% WHF in TSB, e) 10% WHF in TSB.

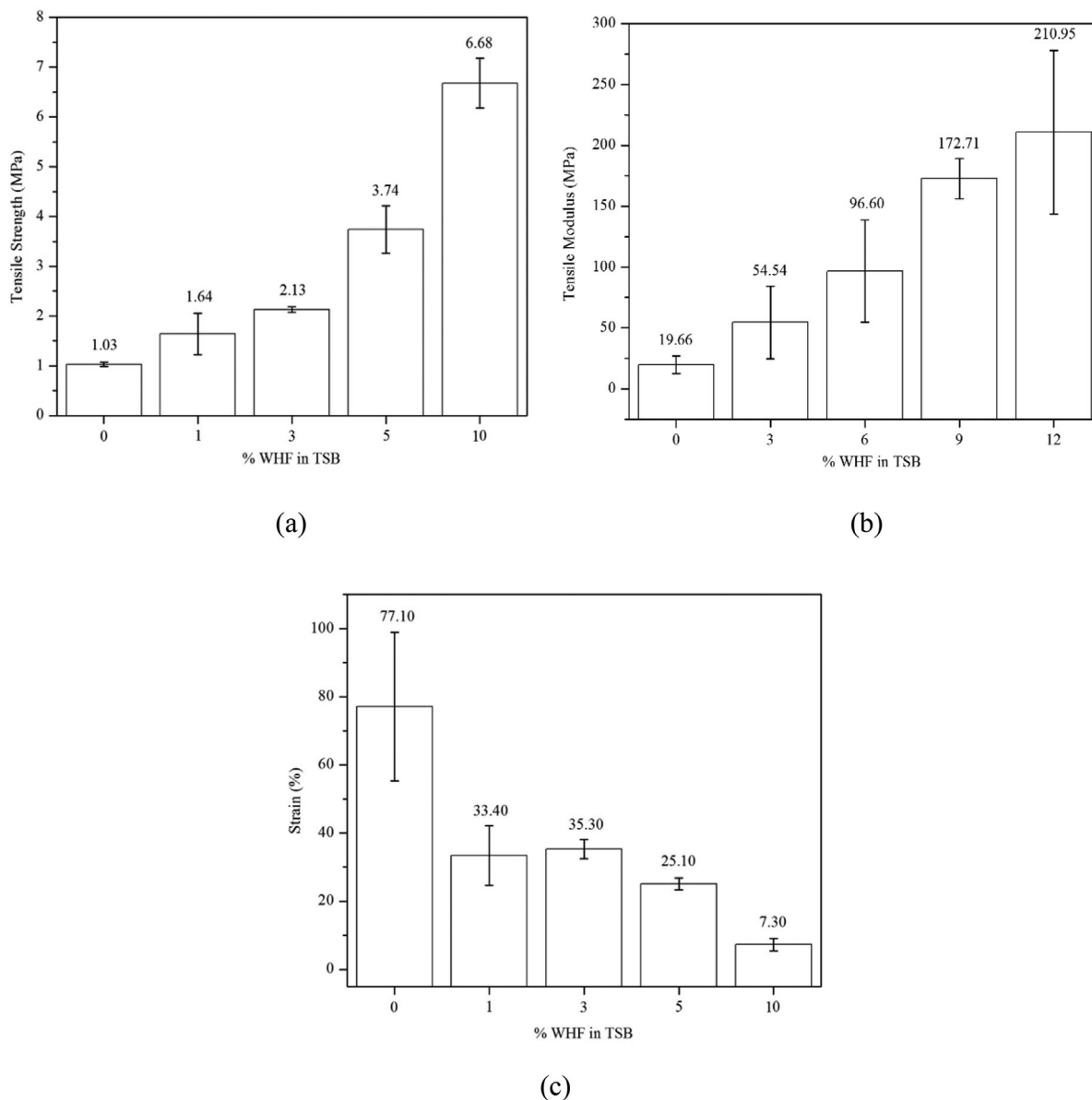


Figure 7. Effect WHF fraction in TSB matrix on mechanical properties of a) tensile strength b) tensile modulus c) fracture strain. Results of five repeats with error bars.

stress from the matrix to the WHF improving mechanical properties of the biocomposite.

4. Conclusions

The present study has highlighted that WHF, a major environmental hazard, could be put to good use in biocomposite production. Chemical and mechanical treatment reduced hemicellulose and lignin content in WHF while increasing cellulose content. The 1–10% fractions of WHF in TSB resulted in an improved material as evidenced by SEM photographs which indicated uniform distribution, and strong, good interfacial bonding. As the amount of WHF in the TSB matrix increased so did tensile properties, tensile modulus, and

thermal and moisture resistance. However, the strain of the biocomposite decreased. The biocomposite of 10% WHF delivered the best performance (improvement of 549% TS, 973% TM), thermal and moisture resistance, and has potential for commercial applications with the appropriate development of technology to achieve this economically.

Acknowledgments

Acknowledgment is addressed to Department of Mechanical Engineering, Andalas University for supporting this research in 2016 (without contract number), and 2017 with contract number 080/UN.16.09.D/PL/2017.

Conflict of Interest

We state that there is no conflict of interest in this research. This research was carried out in the absence of any commercial or financial relationships. In this case, we just want to develop the potential of bioplastic as a substitute for synthetic plastics in laboratory scale. However, as far as we are aware, there are no previous studies investigating the microscale effects of WHF on the physical and mechanical properties of starch tapioca based thermoplastic. Therefore, this research was designed to study the properties of this combination.

Keywords

biocomposites, mechanical properties, tapioca starch biopolymers, thermal and moisture resistance, water hyacinth fiber pulp

Received: October 30, 2017

Revised: January 29, 2018

Published online: April 10, 2018

- [1] L. Averous, N. Boquillon, *Carbohydr. Polym.* **2004**, 56, 111.
- [2] M. N. Angles, A. Dufresne, *Macromolecules* **2000**, 33, 8344.
- [3] E. D. M. Teixeira, D. Pasquini, A. A. Curvelo, E. Corradini, M. N. Belgacem, A. Dufresne, *Carbohydr. Polym.* **2009**, 78, 422.
- [4] X. Cao, Y. Chen, P. R. Chang, A. D. Muir, G. Falk, *Express Polym. Lett.* **2008**, 2, 502.
- [5] Y. Lu, L. Weng, X. Cao, *Carbohydr. Polym.* **2006**, 63, 198.
- [6] K. Majdzadeh-Ardakani, A. H. Navarchian, F. Sadeghi, *Carbohydr. Polym.* **2010**, 79, 547.
- [7] Q. Sun, T. Xi, Y. Li, L. Xiong, *PLoS ONE* **2014**, 9, e106727.
- [8] A. Dufresne, D. Dupeyre, M. R. Vignon, *J. Appl. Polym. Sci.* **2000**, 76, 2080.
- [9] M. Asrofi, H. Abrial, Y. K. Putra, S. M. Sapuan, H. J. Kim, *Int. J. Biol. Macromol.* **2018**, 108, 167.
- [10] H. Abrial, G. J. Putra, M. Asrofi, J. W. Park, H. J. Kim, *Ultrason. Sonochem.* **2018**, 40, 697.
- [11] W. Chen, H. Yu, Y. Liu, P. Chen, M. Zhang, Y. Hai, *Carbohydr. Polym.* **2011**, 83, 1804.
- [12] Z. Q. Fu, M. Wu, X. Y. Han, L. Xu, *Starch/Stärke* **2017**, 69, 1700053.
- [13] J. Prachayawarakorn, A. Hanchana, *Starch/Stärke* **2017**, 69, 1600113.
- [14] J. P. López, P. Mutjé, A. J. F. Carvalho, A. A. S. Curvelo, J. Girones, *Ind. Crop. Prod.* **2013**, 44, 300.
- [15] A. Kaushik, M. Singh, G. Verma, *Carbohydr. Polym.* **2010**, 82, 337.
- [16] C. Miao, W. Y. Hamad, *Cellulose* **2013**, 20, 2221.
- [17] A. Bhattacharya, P. Kumar, *Electron. J. Environ. Agric. Food Chem.* **2010**, 9, 112.
- [18] M. T. Sundari, A. Ramesh, *Carbohydr. Polym.* **2012**, 87, 1701.
- [19] M. A. S. Azizi Samir, F. Alloin, A. Dufresne, *Biomacromolecules* **2005**, 6, 612.
- [20] Q. Cheng, S. Wang, Q. Han, *J. Appl. Polym. Sci.* **2010**, 115, 2756.
- [21] A. Chakraborty, M. Sain, M. Kortschot, *Holzforschung* **2005**, 59, 102.
- [22] F. Fahma, S. Iwamoto, N. Hori, T. Iwata, A. Takemura, *Cellulose* **2010**, 17, 977.
- [23] Y. Chen, C. Liu, P. R. Chang, X. Cao, D. P. Anderson, *Carbohydr. Polym.* **2009**, 76, 607.
- [24] M. Rahimi, R. Behrooz, *Int. J. Polym. Mater.* **2011**, 60, 529.
- [25] B. Khan, K. N. M. Bilal, G. Samin, Z. Jahan, *J. Food. Process Eng.* **2017**, 40, e12447.
- [26] A. G. Supri, H. Ismail, *Polym. Plast. Technol. Eng.* **2011**, 50, 113.
- [27] H. Abrial, D. Kadriadi, A. Rodianus, P. Mastariyanto, S. Arief, S. M. Sapuan, M. R. Ishak, *Mater. Des.* **2014**, 58, 125.
- [28] A. G. Supri, S. J. Tan, H. Ismail, P. L. Teh, *Polym. Plast. Technol. Eng.* **2011**, 50, 898.
- [29] H. Abrial, H. Putra, S. M. Sapuan, M. R. Ishak, *Polym. Plast. Technol. Eng.* **2013**, 52, 446.
- [30] American Society for Testing and Materials, ASTM D882 Standard Test Methods for Tensile Properties of Thin Plastic Sheeting, Annual Book of ASTM standards, Philadelphia 1991.
- [31] L. G. J. M. A. Segal, J. J. Creely, A. E. Martin Jr, C. M. Conrad, *Text. Res. J.* **1959**, 29, 786.
- [32] M. G. Lomeli-Ramírez, S. G. Kestur, R. Manríquez-González, S. Iwakiri, G. B. de Muniz, T. S. Flores-Sahagun, *Carbohydr. Polym.* **2014**, 102, 576.
- [33] N. L. García, L. Ribba, A. Dufresne, M. I. Aranguren, S. Goyanes, *Macromol. Mater. Eng.* **2009**, 294, 169.
- [34] S. Karimi, A. Dufresne, P. M. Tahir, A. Karimi, A. Abdulkhani, *J. Mater. Sci.* **2014**, 49, 4513.
- [35] M. Jonoobi, A. Khazaeian, P. M. Tahir, S. S. Azry, K. Oksman, *Cellulose* **2011**, 18, 1085.
- [36] M. Jonoobi, J. Harun, M. Mishra, K. Oksman, *Bio Resour.* **2009**, 4, 626.
- [37] S. Y. Lee, D. J. Mohan, I. A. Kang, G. H. Doh, S. Lee, S. O. Han, *Fibers Polym.* **2009**, 10, 77.
- [38] H. M. Ng, L. T. Sin, T. T. Tee, S. T. Bee, D. Hui, C. Y. Low, A. R. Rahmat, *Compos. Part B Eng.* **2015**, 75, 176.
- [39] M. Kumar, S. Mohanty, S. K. Nayak, M. R. Parvaiz, *Bioresour. Technol.* **2010**, 101, 8406.
- [40] K. M. Dean, M. D. Do, E. Petinakis, L. Yu, *Compos. Sci. Technol.* **2008**, 68, 1453.
- [41] A. Alemdar, M. Sain, *Bioresour. Technol.* **2008**, 99, 1664.
- [42] K. Kaewtatip, J. Thongmee, *Mater. Des.* **2012**, 40, 314.
- [43] J. Sahari, S. M. Sapuan, E. S. Zainudin, M. A. Maleque, *Mater. Des.* **2013**, 49, 285.
- [44] A. Kaushik, M. Singh, G. Verma, *Carbohydr. Polym.* **2010**, 82, 337.
- [45] M. S. Sreekala, K. Goda, P. V. Devi, *Compos. Interfaces* **2008**, 15, 281.
- [46] Y. Dong, A. Ghataura, H. Takagi, H. J. Haroosh, A. N. Nakagaito, K. T. Lau, *Compos. Part A Appl. Sci. Manuf.* **2014**, 63, 76.
- [47] A. N. Frone, D. M. Panaitescu, D. Donescu, C. I. Spataru, C. Radovici, R. Trusca, R. Somoghi, *Bio Resour.* **2011**, 6, 487.
- [48] P. R. Chang, R. Jian, P. Zheng, J. Yu, X. Ma, *Carbohydr. Polym.* **2010**, 79, 301.